LA--1393

[redacted]

[redacted]

[redacted] c.3

LOS ALAMOS SCIENTIFIC LABORATORY

OF THE

UNIVERSITY OF CALIFORNIA

CONTRACT W-7405-ENG. 36 WITH

U. S. ATOMIC ENERGY COMMISSION

UNCLASSIFIED

[redacted]

[redacted]

UNCLASSIFIED

LOS ALAMOS SCIENTIFIC LABORATORY
of the
UNIVERSITY OF CALIFORNIA

Report written:
March 25, 1952

LA-1393

This document consists of 51 pages

[redacted]

PUBLICLY RELEASABLE
Per J.A. Brown, FSS-16 Date: 11-8-95
By Marcia Bullinger CIC-14 Date: 11-15-95

THEORETICAL EQUATION OF STATE FOR DETONATION PRODUCTS OF SOLID EXPLOSIVES. II. DETONATION VELOCITIES AND CHAPMAN-JOUGET P, V, AND T FOR RDX ASSUMING A FIXED PRODUCT COMPOSITION

by

Wm. W. Wood

W. Fickett

Classification changed to UNCLASSIFIED
by authority of the U. S. Atomic Energy Commission,
Per Charles F. Kessel 12-12-55
By REPORT LIBRARY 1-3-56

[redacted]

Classification changed
by
Report Library
12-18-53

[redacted]

UNCLASSIFIED

[redacted]

UNCLASSIFIED

Distributed: APR 4 1952

LA-1393

Washington Document Room	1 - 7
J R. Oppenheimer	8
Los Alamos Report Library	9 - 30

[redacted]

UNCLASSIFIED

[redacted]

UNCLASSIFIED

ABSTRACT

Detonation velocities computed for RDX by use of a free volume equation of state for mixtures are compared with existing experimental data, and certain possible implications of the comparison are discussed. Numerical tables of the Lennard-Jones and Devonshire equation of state in the high temperature-high density region are presented.

ACKNOWLEDGMENT

Shortly before the preparation of this report we were able to discuss the subject matter with Prof. J. G. Kirkwood, to whom we are grateful for his advice and inspiration.

[redacted]

UNCLASSIFIED

[redacted]

A Theoretical Equation of State for Detonation Products of Solid Explosives. II. Detonation Velocities and Chapman-Jouget P, V, and T for RDX Assuming a Fixed Product Composition

Introduction:

This is an interim report on the theoretical aspects of the current equation of state program in GMX. It is the second member of the series begun with the report by Zevi W. Salsburg[1]. A revised and corrected version of this latter report will be issued shortly.

The numerical calculations presented here supplant those of Section D of reference (1). As mentioned in the latter the available tables were not well adapted to detonation calculations, and the calculations reported there were unavoidably inaccurate. Section I describes briefly the extension of the equation of state tables which was so evidently needed. Section 2 is devoted to the present numerical procedure, while Section 3 describes the results obtained for the explosive RDX. In Section 4 these results are discussed and our future program outlined.

---

[1] "An Equation of State for Fluid Mixtures," dated September 4, 1951, issued by GMX-2.

[redacted]

Section 1.

Tables Of The Lennard-Jones And Devonshire Equation Of State At High Temperatures And Densities

The Lennard-Jones and Devonshire equation of state has been presented in tabular form by Wentorff, et al[2]. These tables are not sufficient for our purposes for two reasons: They do not extend to sufficiently low values of the reduced volume, and the intervals in both reduced temperature and reduced volume are unsatisfactory for interpolation in the region of interest to us.

Accordingly, we have prepared a tabulation of the equation of state which extends to lower reduced volumes and covers the region of interest with considerably finer intervals in reduced temperature and more regular intervals in reduced volume. The potential of intermolecular force was the same as that used in reference (2), $V(r) = 4\epsilon^*\left[\left(\frac{r_0}{r}\right)^{12} - \left(\frac{r_0}{r}\right)^{6}\right]$. The calculations were quite similar to those described there, and were carried out on an International Business Machines Corporation Model II CPEC combination. The numerical integrations were carried out with Simpson's rule and a nominal 64 to 72 values of the integrand. Shortening of the range of integration was carried out as required so that the number of non-negligible values was always at least two-thirds of the nominal

---

[2] R. H. Wentorff, R. J. Buehler, J. O. Hirschfelder, and C. F. Curtiss, J. Chem. Phys. 18, 1484 (1950)

[redacted]

[redacted]

number. Thus these results are somewhat more accurate than those of Wentorff, et al, who state that they used Simpson's rule with 15 to 30 non-negligible values of the integrand. A rough estimate of the error involved in the numerical evaluation of the integrals was obtained by comparing the results with those obtained by using Simpson's rule with half the original number of points. The number of figures to be included in the tabular entries was decided on the basis of this comparison. Although the last figure in each entry is thought to have some significance, it is not necessarily a "significant figure" in the strict sense.

The results of the calculation are presented in Tables I - VI. The reduced volume and temperature are defined as follows: $\tau = \frac{v}{v^*}$ and $\theta = \frac{kT}{\epsilon^*}$, where $v^* = N_A r_0^3$ (N_A being Avogadro's number) and ϵ^* are the molecular parameters defining the Lennard-Jones potential of intermolecular force. The symbols G, g_1, and g_m represent integrals needed for the evaluation of the compressibility factor $\mathcal{H} = \frac{pv}{NkT}$, the reduced internal energy of gas imperfection $\mathcal{E}' = \frac{E'}{N\epsilon^*}$, and the reduced entropy of gas imperfection S'/Nk. Precise definitions of and expressions for these quantities may be found in reference (2).[3]

To facilitate interpolation, tables of $\mathcal{H}\theta$, log $(\mathcal{H}-1)$ and log $\mathcal{E}'$ were prepared. With these, five-point interpolation in τ and three-point interpolation in θ gave satisfactory results.

---

[3] It should be noted that Eq. (21) of reference (2) is incorrect. The correct expression for the entropy is

(Continued on Page 7)

[redacted]

[redacted]

$$S = S^{\circ}(T) - N_A k \log (NkT/v_0^*) + N_A k \log (v/v^*)$$

$$+ S'(v,T) + N_A k \log (\sigma/e) + N_A kT \frac{\partial \log \sigma}{\partial T}$$

$$S'(v,T) = (12 N_A \epsilon^*/T)\left[(v^*/v)^4 (g_L/G) - 2(v^*/v)^2 (g_m/G)\right]$$

$$+ Nk \log (G/G_\infty)$$

$$G_\infty = \lim_{v \to \infty} G = (2\sqrt{2}\,\pi)^{-1}$$

The parameter σ has been precisely defined by Kirkwood, J. Chem. Phys. 18, 380 (1950). It has the property:

$$\lim_{v \to \infty} \sigma = e$$

$$\lim_{v \to 0} \sigma = 0$$

each limit presumably being approached with zero slope.

Thus the error in Eq. (21) of reference (2) is approximately $(-N_A k)$ in the region of present interest, where σ is probably close to one.

[redacted]

[redacted]

Table I. A tabulation of G

θ \ T	.30	.35	.40	.45	.50
20	1.3974 (-5)	3.5436 (-5)	7.8929 (-5)	1.5865 (-4)	2.9305 (
30	2.5404 (-5)	6.3[illegible]53 (-5)	1.4045 (-4)	2.7771 (-4)	5.0264 (
40	3.8708 (-5)	9.6496 (-5)	2.0983 (-4)	4.0887 (-4)	7.2740 (
50	5.3540 (-5)	1.3245 (-4)	2.8498 (-4)	5.4811 (-4)	9.6080 (
60	6.9688 (-5)	1.7110 (-4)	3.6454 (-4)	6.9284 (-4)	1.19891 (
70	8.6961 (-5)	2.1199 (-4)	4.4753 (-4)	8.4152 (-4)	1.43935 (
80	1.0522 (-4)	2.5478 (-4)	5.3326 (-4)	9.9289 (-4)	1.68059 (
90	1.2437 (-4)	2.9919 (-4)	6.2108 (-4)	1.14608 (-3)	1.92159 (
100	1.4432 (-4)	3.4500 (-4)	7.1075 (-4)	1.30046 (-3)	2.1612 (
110	1.6498 (-4)	3.9203 (-4)	8.0182 (-4)	1.45555 (-3)	2.3997 (
120	1.8630 (-4)	4.4012 (-4)	8.9403 (-4)	1.61097 (-3)	2.6362 (
130	2.0821 (-4)	4.8914 (-4)	9.8713 (-4)	1.76643 (-3)	2.8707 (
140	2.3067 (-4)	5.3898 (-4)	1.08095 (-3)	1.92172 (-3)	3.1029 (
150	2.5362 (-4)	5.8953 (-4)	1.17533 (-3)	2.07666 (-3)	3.3327 (

Note: The number in parentheses is the power of 10 by which the entry is to be multiplied.

Table I. (continued)

θ \ τ	.55	.60	.65	.70	.80
20	5.0377 (-4)	8.1403 (-4)	1.24644 (-3)	1.8205 (-3)	3.4501
30	8.4415 (-4)	1.32997 (-3)	1.98348 (-3)	2.8203 (-3)	5.0760
40	1.19892 (-3)	1.85204 (-3)	2.7068 (-3)	3.7754 (-3)	6.5537
50	1.55874 (-3)	2.3690 (-3)	3.4085 (-3)	4.6825 (-3)	7.9083
60	1.91891 (-3)	2.8770 (-3)	4.0857 (-3)	5.5442 (-3)	9.1606
70	2.2762 (-3)	3.3738 (-3)	4.7385 (-3)	6.3641 (-3)	1.03269
80	2.6299 (-3)	3.8586 (-3)	5.3679 (-3)	7.1462 (-3)	1.14198
90	2.9787 (-3)	4.3313 (-3)	5.9703 (-3)	7.8941 (-3)	1.24492
100	3.3222 (-3)	4.7920 (-3)	6.56201 (-3)	8.6107 (-3)	1.34231
110	3.6602 (-3)	5.2412 (-3)	7.12946 (-3)	9.2991 (-3)	1.43481
120	3.9924 (-3)	5.6793 (-3)	7.67894 (-3)	9.9615 (-3)	1.52294
130	4.3191 (-3)	6.1068 (-3)	8.21164 (-3)	1.06001 (-2)	1.60715
140	4.6401 (-3)	6.5241 (-3)	8.72865 (-3)	1.12168 (-2)	1.68783
150	4.9556 (-3)	6.9317 (-3)	9.23098 (-3)	1.18133 (-2)	1.76529

[redacted]

Table I. (continued)

θ \ T	.90	1.00	1.10	1.20	1.30
20	5.7596 (-3)	8.72641 (-3)	1.22723 (-2)	1.62921 (-2)	2.06759 (
30	8.08891 (-3)	1.17704 (-2)	1.59936 (-2)	2.06249 (-2)	2.55424 (
40	1.01207 (-2)	1.43411 (-2)	1.90591 (-2)	2.41280 (-2)	2.94228 (
50	1.19315 (-2)	1.65830 (-2)	2.16889 (-2)	2.70963 (-2)	3.26809 (
60	1.35709 (-2)	1.85805 (-2)	2.40040 (-2)	2.96860 (-2)	3.55046 (
70	1.50726 (-2)	2.03877 (-2)	2.60793 (-2)	3.19914 (-2)	3.80053 (
80	1.64611 (-2)	2.20419 (-2)	2.79646 (-2)	3.40741 (-2)	4.02550 (
90	1.77543 (-2)	2.35698 (-2)	2.96952 (-2)	3.59770 (-2)	4.23034 (
100	1.89661 (-2)	2.49913 (-2)	3.12969 (-2)	3.77313 (-2)	4.41861 (
110	2.01075 (-2)	2.63220 (-2)	3.27894 (-2)	3.93603 (-2)	4.59299 (
120	2.11870 (-2)	2.75739 (-2)	3.41879 (-2)	4.08823 (-2)	4.75552 (
130	2.22120 (-2)	2.87568 (-2)	3.55046 (-2)	4.23114 (-2)	4.90782 (
140	2.31881 (-2)	2.98787 (-2)	3.67494 (-2)	4.36592 (-2)	5.05117 (
150	2.41205 (-2)	3.09460 (-2)	3.79304 (-2)	4.49352 (-2)	5.18662 (

Table II. A tabulation of g_L

θ \ τ	.30	.35	.40	.45	.50
20	2.915 (-7)	1.3736 (-6)	5.2184 (-6)	1.6717 (-5)	4.6548 (-5
30	7.890 (-7)	3.6668 (-6)	1.3653 (-5)	4.2604 (-5)	1.1501 (-4
40	1.5917 (-6)	7.3604 (-6)	2.6693 (-5)	8.1459 (-5)	2.1441 (-4
50	2.7353 (-6)	1.33344 (-5)	4.4543 (-5)	1.3329 (-4)	3.4339 (-4
60	4.2442 (-6)	1.89891 (-5)	6.7288 (-5)	1.9791 (-4)	5.0042 (-4
70	6.1402 (-6)	2.7177 (-5)	9.4943 (-5)	2.7491 (-4)	6.8395 (-4
80	8.4400 (-6)	3.6964 (-5)	1.2748 (-4)	3.6393 (-4)	8.9258 (-4
90	1.1157 (-5)	4.8375 (-5)	1.6487 (-4)	4.5455 (-4)	1.1250 (-3
100	1.4306 (-5)	6.1422 (-5)	2.0699 (-4)	5.7638 (-4)	1.3786 (-3
110	1.768[illegible] (-5)	7.6108 (-5)	2.5380 (-4)	6.9901 (-4)	1.6540 (-3
120	2.1915 (-5)	9.2432 (-5)	3.0519 (-4)	8.3210 (-4)	1.9493 (-3
130	2.6392 (-5)	1.10389 (-4)	3.6108 (-4)	9.7527 (-4)	2.2637 (-3
140	3.1324 (-5)	1.29908 (-4)	4.2137 (-4)	1.12821 (-3)	2.5962 (-3
150	3.6714 (-5)	1.51152 (-4)	4.8598 (-4)	1.29060 (-3)	2.9459 (-3

Table II. (continued)

θ \ τ	.55	.60	.65	.70	.80
20	1.1524 (-4)	2.5793 (-4)	5.2951 (-4)	1.0086 (-3)	3.0394 (
30	2.7506 (-4)	5.9368 (-4)	1.1759 (-3)	2.1571 (-3)	6.0754 (
40	4.9901 (-4)	1.0485 (-3)	2.0175 (-3)	3.6121 (-3)	9.7168 (
50	7.8180 (-4)	1.6056 (-3)	3.0279 (-3)	5.3167 (-3)	1.38230 (
60	1.1188 (-3)	2.2554 (-3)	4.1820 (-3)	7.2302 (-3)	1.83034 (
70	1.5035 (-3)	2.9873 (-3)	5.4618 (-3)	9.3229 (-3)	2.30952 (
80	1.9344 (-3)	3.7932 (-3)	6.8527 (-3)	1.15716 (-2)	2.81516 (
90	2.4072 (-3)	4.6664 (-3)	8.3431 (-3)	1.39583 (-2)	3.34377 (
100	2.9189 (-3)	5.6012 (-3)	9.9233 (-3)	1.64681 (-2)	3.89256 (
110	3.4669 (-3)	6.5927 (-3)	1.15852 (-2)	1.90890 (-2)	4.45932 (
120	4.0499 (-3)	7.6364 (-3)	1.33220 (-2)	2.18109 (-2)	5.04222 (
130	4.6627 (-3)	8.7287 (-3)	1.51277 (-2)	2.46253 (-2)	5.63973 (
140	5.3066 (-3)	9.8663 (-3)	1.69972 (-2)	2.75244 (-2)	6.25058 (
150	5.9788 (-3)	1.1046 (-2)	1.89261 (-2)	3.05021 (-2)	6.87366 (

[redacted]

Table II. (continued)

θ \ τ	.90	1.00	1.10	1.20	1.30
20	7.5301 (-3)	1.60831 (-2)	3.06599 (-2)	5.35096 (-2)	8.71106
30	1.41960 (-2)	2.88684 (-2)	5.28479 (-2)	8.92163 (-2)	1.41328
40	2.18513 (-2)	4.30695 (-2)	7.68762 (-2)	1.27150 (-1)	1.98096
50	3.02361 (-2)	5.82858 (-2)	1.02203 (-1)	1.66643 (-1)	2.56648
60	3.91918 (-2)	7.42830 (-2)	1.28518 (-1)	2.07319 (-1)	3.16553
70	4.86127 (-2)	9.09037 (-2)	1.55623 (-1)	2.48936 (-1)	3.77536
80	5.84236 (-2)	1.08056 (-1)	1.83381 (-1)	2.91330 (-1)	4.39407
90	6.85684 (-2)	1.25647 (-1)	2.11691 (-1)	3.34381 (-1)	5.02027
100	7.90041 (-2)	1.43622 (-1)	2.40479 (-1)	3.77997 (-1)	5.65289
110	8.95964 (-2)	1.61935 (-1)	2.69685 (-1)	4.22108 (-1)	6.29103
120	1.00617 (-1)	1.80547 (-1)	2.99260 (-1)	4.66657 (-1)	6.93391
130	1.11745 (-1)	1.99428 (-1)	3.29168 (-1)	5.11597 (-1)	7.58078
140	1.23059 (-1)	2.18552 (-1)	3.59375 (-1)	5.56886 (-1)	8.23090
150	1.34544 (-1)	2.37897 (-1)	3.89854 (-1)	6.02489 (-1)	8.88354

Table III. A tabulation of g_M

θ \ τ	.30	.35	.40	.45	.50
20	6.894 (-8)	3.2222 (-7)	1.2095 (-6)	3.812 (-6)	1.0392 (
30	1.8573 (-7)	8.531 (-7)	3.123 (-6)	9.531 (-6)	2.5026 (
40	3.7304 (-7)	1.6852 (-6)	6.033 (-6)	1.7913 (-5)	4.5609 (
50	6.381 (-7)	2.8374 (-6)	9.953 (-6)	2.8855 (-5)	7.1572 (
60	9.859 (-7)	4.3197 (-6)	1.4876 (-5)	4.2222 (-5)	1.02385 (
70	1.4204 (-6)	6.140 (-6)	2.0779 (-5)	5.7859 (-5)	1.37574 (
80	1.9445 (-6)	8.295 (-6)	2.7634 (-5)	7.5624 (-5)	1.7674 (
90	2.5602 (-6)	1.0787 (-5)	3.5413 (-5)	9.5381 (-5)	2.1957 (
100	3.270 (-6)	1.3612 (-5)	4.4074 (-5)	1.17003 (-4)	2.6517 (
110	4.073 (-6)	1.6766 (-5)	5.3587 (-5)	1.40377 (-4)	3.1396 (
120	4.972 (-6)	2.0244 (-5)	6.3921 (-5)	1.65402 (-4)	3.6542 (
130	5.966 (-6)	2.4041 (-5)	7.5041 (-5)	1.9199 (-4)	4.1932 (
140	7.055 (-6)	2.8150 (-5)	8.6918 (-5)	2.2006 (-4)	4.7547 (
150	8.240 (-6)	3.2566 (-5)	9.9521 (-5)	2.4954 (-4)	5.3368 (

[redacted]

Table III. (continued)

θ \ τ	.55	.60	.65	.70	.80
20	2.5078 (-5)	5.4482 (-5)	1.08159 (-4)	1.9861 (-4)	5.5221 (
30	5.7922 (-5)	1.2047 (-4)	2.2925 (-4)	4.0236 (-4)	1.03250 (
40	1.02150 (-4)	2.0578 (-4)	3.7798 (-4)	5.4465 (-4)	1.56569
50	1.56114 (-4)	3.0583 (-4)	5.4849 (-4)	9.1384 (-4)	2.12982
60	2.1855 (-4)	4.1848 (-4)	7.3538 (-4)	1.20241 (-3)	2.71274
70	2.8757 (-4)	5.4130 (-4)	9.3511 (-4)	1.50539 (-3)	3.3071
80	3.6306 (-4)	6.7260 (-4)	1.14508 (-3)	1.81925 (-3)	3.9081
90	4.4394 (-4)	8.1102 (-4)	1.36332 (-3)	2.14141 (-3)	4.5126
100	5.2957 (-4)	9.5550 (-4)	1.58829 (-3)	2.46993 (-3)	5.1184
110	6.1938 (-4)	1.10520 (-3)	1.81879 (-3)	2.80336 (-3)	5.7240
120	7.1290 (-4)	1.25931 (-3)	2.05384 (-3)	3.14053 (-3)	6.3283
130	8.0974 (-4)	1.41726 (-3)	2.29266 (-3)	3.4806 (-3)	6.9304
140	9.0954 (-4)	1.57855 (-3)	2.53461 (-3)	3.8227 (-3)	7.5297
150	1.01200 (-3)	1.74275 (-3)	2.77915 (-3)	4.1664 (-3)	8.1260

Table III. (continued)

θ \ τ	.90	1.00	1.10	1.20	1.30
20	1.25428 (-3)	2.44759 (-3)	4.2568 (-3)	6.7768 (-3)	1.00706
30	2.16755 (-3)	4.0252 (-3)	6.6656 (-3)	1.01877 (-2)	1.46335
40	3.16732 (-3)	5.6100 (-3)	9.0035 (-3)	1.34103 (-2)	1.88551
50	4.1651 (-3)	7.1766 (-3)	1.12621 (-2)	1.64686 (-2)	2.28061
60	5.1671 (-3)	8.7158 (-3)	1.34441 (-2)	1.93850 (-2)	2.65357
70	6.1661 (-3)	1.02245 (-2)	1.55549 (-2)	2.21780 (-2)	3.00795
80	7.1580 (-3)	1.17019 (-2)	1.76005 (-2)	2.48627 (-2)	3.34642
90	8.1406 (-3)	1.31487 (-2)	1.95861 (-2)	2.74512 (-2)	3.67104
100	9.1126 (-3)	1.45659 (-2)	2.15168 (-2)	2.99536 (-2)	3.98344
110	1.00733 (-2)	1.59549 (-2)	2.33969 (-2)	3.23783 (-2)	4.28494
120	1.10224 (-2)	1.73170 (-2)	2.54301 (-2)	3.47323 (-2)	4.57062
130	1.19599 (-2)	1.86535 (-2)	2.70200 (-2)	3.70217 (-2)	4.85935
140	1.28858 (-2)	1.99658 (-2)	2.87695 (-2)	3.92517 (-2)	5.13386
150	1.38003 (-2)	2.12549 (-2)	3.04813 (-2)	4.14267 (-2)	5.40078

Table IV. The compressibility factor pv/NkT

θ \ T	.30	.35	.40	.45	.50
20	140.759	76.064	45.323	29.329	20.387
30	96.145	52.977	32.423	21.6791	15.625
40	73.819	41.400	25.925	17.7938	13.172
50	60.411	34.431	21.9935	15.4224	11.655
60	51.459	29.766	19.3490	13.8142	10.612
70	45.056	26.4227	17.4419	12.6433	9.845
80	40.245	23.9022	15.9972	11.7491	9.253
90	36.498	21.9324	14.8630	11.0408	8.780
100	33.495	20.3487	13.9455	10.4641	8.389
110	31.032	19.0462	13.1866	9.9838	8.061
120	28.976	17.9551	12.5475	9.5767	7.782
130	27.231	17.0267	12.0011	9.2265	7.539
140	25.733	16.2266	11.5277	8.9214	7.326
150	24.431	15.5291	11.1131	8.6528	7.137

Table IV. (continued)

θ \ τ	.55	.60	.65	.70	.80
20	15.084	11.7672	9.5937	8.1066	6.265
30	11.9874	9.6722	8.1260	7.0330	5.635
40	10.3598	8.5444	7.3015	6.4150	5.247
50	9.3357	7.8145	6.7618	5.9987	4.974
60	8.6224	7.2977	6.3715	5.6921	4.765
70	8.0861	6.9066	6.0717	5.4535	4.601
80	7.6689	6.5971	5.8317	5.2605	4.466
90	7.3315	6.3442	5.6337	5.0997	4.351
100	7.0516	6.1324	5.4664	4.9630	4.253
110	6.8144	5.9516	5.3224	4.8447	4.166
120	6.6102	5.7945	5.1968	4.7408	4.090
130	6.4318	5.6566	5.0858	4.6486	4.022
140	6.2742	5.5340	4.9867	4.5660	3.961
150	6.1337	5.4241	4.8974	4.4913	3.905

[redacted]

Table IV. (continued)

θ \ τ	.90	1.00	1.10	1.20	1.30
20	5.2018	4.51787	4.04135	3.65940	3.418
30	4.7897	4.22220	3.81596	3.50972	3.370
40	4.5176	4.01831	3.65450	3.37715	3.158
50	4.3200	3.86564	3.53141	3.27457	3.071
60	4.16681	3.74564	3.43360	3.19198	3.000
70	4.04293	3.64735	3.35722	3.12344	2.940
80	3.93975	3.56479	3.28376	3.06522	2.890
90	3.85187	3.49399	3.22479	3.01486	2.846
100	3.77568	3.43229	3.17319	2.97065	2.807
110	3.70871	3.37781	3.12746	2.93137	2.773
120	3.64915	3.32918	3.08652	2.89613	2.742
130	3.59568	3.28537	3.04955	2.86423	2.714
140	3.54727	3.24559	3.01592	2.83513	2.688
150	3.50314	3.20924	2.98512	2.80843	2.664

[redacted]

Table V. The reduced internal energy of gas imperfection $E'/N\epsilon^*$

θ \ τ	.30	.35	.40	.45	.50
20	617.34	315.44	175.30	104.53	66.328
30	632.32	329.52	[illegible]	117.37	78.390
40	646.61	343.30	[illegible]	129.65	89.811
50	660.75	356.79	214.67	141.47	100.705
60	674.70	370.02	227.60	152.91	111.177
70	688.50	383.06	[illegible]	164.00	121.294
80	702.15	395.86	[illegible]	174.78	131.112
90	715.65	408.45	267.48	185.30	140.673
100	729.07	420.86	273.82	195.58	149.93
110	742.30	433.09	284.95	205.65	159.01
120	755.41	445.00	295.90	215.53	167.90
130	768.40	457.06	301.66	225.23	176.61
140	781.28	468.82	317.27	234.78	185.17
150	794.05	480.44	327.72	244.17	193.58

Table V. (continued)

θ \ T	.55	.60	.65	.70	.80
20	44.554	31.[illegible]	26.398	18.112	13.0[illegible]
30	55.793	41.947	33.857	27.004	19.66
40	66.323	51.665	41.943	35.219	26.70
50	76.333	60.803	50.347	42.955	33.33
60	85.928	69.543	58.355	50.321	39.65
70	95.104	77.942	66.045	57.394	45.73
80	104.010	86.057	73.471	64.226	51.61
90	112.657	93.928	80.672	70.852	57.32
100	121.076	101.588	87.679	77.301	62.88
110	129.293	109.064	94.516	83.596	68.31
120	137.330	116.370	101.202	89.754	73.64
130	145.204	123.527	107.753	95.790	78.86
140	152.930	130.550	114.180	101.714	83.99
150	160.521	137.448	120.497	107.538	89.03

Table V. (continued)

θ \ τ	.90	1.00	1.10	1.20	1.
20	8.8603	6.9966	5.7941	4.9620	4.35
30	15.4864	12.8358	11.0137	9.6879	8.68
40	21.6171	18.2619	15.8873	14.1211	12.75
50	27.406	23.4027	20.5202	18.3486	16.65
60	32.939	28.3285	24.9709	22.4193	20.41
70	38.268	33.0836	29.2760	26.3644	24.06
80	43.431	37.6980	33.4610	30.2051	27.62
90	48.452	42.1935	37.5439	33.9570	31.10
100	53.352	46.5863	41.5387	37.6319	34.52
110	58.145	50.8891	45.4559	41.2389	37.87
120	62.845	55.1121	49.3041	44.7853	41.16
130	67.460	59.2635	53.0904	48.2770	44.40
140	72.000	63.3500	56.8205	51.7189	47.60
150	76.469	67.3775	60.4994	55.1147	50.74

Table VI. The reduced entropy of gas imperfection S'/Nk

θ τ	.30	.35	.40	.45	.5
20	7.5145	6.6025	5.8279	5.1649	4.59
30	6.9274	6.0310	5.2785	4.6456	4.10
40	6.5161	5.6346	4.9018	4.2899	3.77
50	6.2005	5.3334	4.6181	4.0260	3.53
60	5.9461	5.0921	4.3924	3.8174	3.34
70	5.7335	4.8910	4.2062	3.6465	3.18
80	5.5512	4.7202	4.0485	3.5025	3.05
90	5.3922	4.5719	3.9121	3.3786	2.94
100	5.2509	4.4411	3.7926	3.2702	2.84
110	5.1248	4.3246	3.6865	3.1742	2.75
120	5.0107	4.2200	3.5912	3.0883	2.68
130	4.9068	4.1243	3.5050	3.0106	2.61
40	4.8113	4.0371	3.4264	2.9399	2.54
50	4.7232	3.9570	3.3543	2.8750	2.49

Table VI. (continued)

θ \ τ	.55	.60	.65	.70	.8
20	4.1065	3.6852	3.3216	3.0069	2.4945
30	3.6498	3.2617	2.9289	2.64517	2.1942
40	3.3463	2.9817	2.67319	2.40846	1.9[illegible]13
50	3.1229	2.7778	2.48549	2.2356[illegible]	1.8[illegible]32
60	2.9478	2.6184	2.33939	2.10129	1.717
70	2.80653	2.48885	2.22079	1.99221	1.6241
80	2.68756	2.38046	2.1216	1.90096	1.5456
90	2.58569	2.28773	2.03676	1.82290	1.4783
100	2.49697	2.20701	1.96291	1.75493	1.4197
110	2.41863	2.13575	1.89774	1.69493	1.3679
120	2.34869	2.07216	1.83955	1.64134	1.3216
130	2.28566	2.01487	1.78711	1.59302	1.2793
140	2.22840	1.96283	1.73947	1.54911	1.2418
150	2.17602	1.91523	1.69589	1.50893	1.2069

Table VI. (continued)

θ \ T	.90	1.00	1.10	1.20	1.
20	2.09945	1.78771	1.53613	1.3[illegible]891	1.1[illegible]5
30	1.82995	1.55025	1.32391	1.13680	0.[illegible]79
40	1.65331	1.39392	1.18351	1.00910	.861
50	1.52400	1.27911	1.08055	0.91469	.774
60	1.42307	1.18925	0.99886	.84044	.706
70	1.34088	1.11592	.93247	.77960	.649
80	1.27193	1.05428	.87657	.72830	.602
90	1.21277	1.00132	.82847	.68410	.561
100	1.16114	0.95503	.78637	.64537	.525
110	1.11544	.91401	.74903	.61099	.493
120	1.07455	.87726	.71555	.58013	.464
130	1.03760	.84403	.68524	.55218	.438
140	1.00396	.81374	.65759	.52667	.415
150	0.97312	.78596	.63221	.50324	.393

Section 2.

Calculation of Detonation Velocity with the Free Volume Equation of State.

The method of reference (1) has been somewhat modified and is briefly described in the following. The Hugoniot equation can be written in the reduced variables as

$$\frac{\bar{C}_v^o(T)}{R}\theta + \mathcal{E}' - \frac{Q}{N_A\bar{\epsilon}^*} - \frac{1}{2}\mathcal{H}\theta(\tau_o/\tau - 1) \qquad (2\text{-}1)$$

where

$$Q = -\sum_i x_i \Delta H^o_{f_i} + \frac{M}{M_o}\Delta H_{f_o} + H^o(T_o) \qquad (2\text{-}2)$$

$$\bar{C}_v^o(T) = \frac{E^o(T) - E^o(0)}{T} \qquad (2\text{-}3)$$

and

$$\tau_o = \frac{M/\rho_o}{\bar{v}^*} \qquad (2\text{-}4)$$

We consider here only the case in which all of the products are gaseous. All extensive thermodynamic functions are taken for one mole of the gaseous mixture, or one mole of pure component i as appropriate. Here x_i is the mole fraction of component i in the final state; ΔH^o_{fi} is the standard molar enthalpy of formation of component i at T_o, ΔH^o_{fo} that of the explosive; M_o is the molecular weight of the explosive, and M is the mass of explosive producing one mole of product gas. $H^o(T)$ and $E^o(T)$ denote the molar enthalpy and internal energy of the product gas (with composition fixed at the x_i) at infinite volume at temperature T. The initial explosive density is denoted by ρ_o . The reduced variables τ, θ, $\mathcal{H}$, and $\mathcal{E}'$ are defined as Section 1, except that v^* and ϵ^* are replaced by $\bar{v}^*$ and $\bar{\epsilon}^*$ as in reference (1).

[redacted] [redacted]

The detonation velocity $\mathcal{D}$ corresponding to this transition is given by

$$\mathcal{D}^2 = \frac{N_A \bar{\epsilon}^*}{M} \frac{\tau_0^2}{\tau^2} \frac{\mathcal{H}\theta}{\frac{\tau_0}{\tau} - 1} \tag{2-5}$$

The Chapman-Jouget condition may be stated as

$$D = \min \mathcal{D} \quad \text{with} \quad \tau_0/\tau > 1 \tag{2-6}$$

D being the actual steady detonation velocity achieved.

We note that $\bar{v}*$ does not appear explicitly in (1) and (5). Thus for a given explosive and an assumed fixed composition in the final state (the equations for chemical equilibrium cannot be written in reduced form without explicit appearance of $\bar{v}*$ except in special cases) D can be found as a function of two independent variables τ_0 and $N_A\bar{\epsilon}*$. Comparison with experiment cannot be made without relating τ_0 to ρ_0 by (4), which contains $\bar{v}*$, but this transformation is easily made, and it is a considerable simplification that (1), (5), and (6) do not have to be solved for each different $\bar{v}*$.

The present numerical procedure is as follows. For a given and $N_A\bar{\epsilon}*$, three or four equally spaced values of τ known from experience to bracket the C-J value are selected. The required interval in τ is smaller than the tabular interval, so that the interpolation procedures mentioned in the preceding section are used in obtaining corresponding values of the dependent variables. Equation (2-1) is then solved for θ at each of these values of τ. To do this it has been found satisfactory to evaluate the left hand side of (2-1) for the three tabular values of θ closest to the solution, then finding by three point Lagrangian interpolation the value of θ which

[redacted]

[redacted]

have a section of the Hugoniot curve, with values of $\mathcal{T}$, $\mathcal{H}$, and $\mathcal{D}$ (from (2-5)) known for each $\mathcal{T}$. The minimum $\mathcal{D} = D$ and the corresponding values of $\mathcal{T}$, $\mathcal{H}$, etc. are then found by Lagrangian interpolation.

No calculations have been made to date for other than fixed composition. The procedure when chemical equilibrium is assumed will be appreciably more complicated. The procedure presently used requires about 2-1/2 hours per pair of values of $\mathcal{T}_0$ and $N\bar{\epsilon}*$ when a desk calculator is used. The method has been adapted to the IBM CPEC Model II combination; on this, exclusive of set-up time, about 15 minutes are required.

[redacted] [redacted]

Calculations for RDX

At present calculations have been made for only one explosive, RDX, $(CH_2NNO_2)_3$, cyclotrimethylenetrinitramine. This explosive was chosen on the recommendation of E. H. Eyster because it is the member of the family of explosives having composition balanced to CO, H_2O, and N_2 for which the most extensive experimental detonation velocity measurements have been made. The balanced composition was considered desirable because it was felt that it would permit greater certainty about the composition than in other cases.

In our calculations we have used the values of the physical constants and the ideal gas values of the thermodynamic functions of the various component gases as tabulated by the National Bureau of Standards.[4] We have assumed the decomposition to be to CO, H_2O, and N_2; corresponding to this process we used $Q = 31.482 \frac{\text{Kcal}}{\text{mole gas}}$, using a value for the internal energy of combustion of -501.82 Kcal/mole RDX.[5] We have taken T_0 as 25°C.

As discussed in reference (1), and as will be seen later in this report, there are many reasons for suspecting that the Lennard-Jones (6,12) intermolecular potential may not adequately represent the actual situation in the region of internuclear distances attained in detonation, particularly if the same constants $N_A\epsilon*$ and $v*$ as found from the usual low temperature

---

[4] N.B.S. "Selected Values of Chemical Thermodynamic Properties."

[5] We have lately learned (private communication, D.V.Sickman to L.C.Smith) that this figure is actually the National Bureau of Standards ΔH of combustion. This gives $Q = 31.877$ Kcal/mole.

[redacted]

[redacted]

viscosity and virial coefficient date are used. (These latter lead to the values $N_A\bar{\epsilon}* = 224 \frac{\text{cal}}{\text{mole}}$, $\bar{v}* = 25.48 \frac{\text{cm}^3}{\text{mole}}$). Thus we are led to first inquire as to whether values of $N_A\bar{\epsilon}*$ and $\bar{v}*$ can be found such that the calculated detonation velocities adequately represent those obtained experimentally throughout the loading density range. Under our assumption of fixed composition this can be done without regard to the question of assigning individual values to the $N_A\epsilon_i^*$ and v_i*.

As mentioned in Section 2 it is most convenient to compute D as a function of τ_0 and $N_A\bar{\epsilon}*$. The results are shown in Table 7. Our present comparison with experiment is based on the interpretation of the RDX data in OSRD 5611 in terms of a linear relation between the infinite-diameter rate and the loading density ρ_0[6]. Work is underway in GMX-2 and GMX-8 to determine the validity of this assumption, particularly in the high density range. For the present, however, we use

$$D_{exp} = 2597 + 3540\,\rho_0 \text{ m/sec.} \quad (\rho_0 \text{ in g/cm}^3) \tag{3-1}$$

The standard deviation of the experimental points from (3-1) is estimated to be about 50 m/sec. However, the only experimental points for densities greater than 1.52 g/m^3 are the three small charges of very high density (1.77 g/m^3) obtained by GMX-2 and GMX-8. When corrected for diameter effect according to reference (5b), they fall about 170 m/sec. below Equation (3-1). The high density region is accordingly poorly defined experimentally.

Equation (3-1) may be written, by use of (2-4) in the form

$$D_{exp} = 2597 + 3540\,\frac{M}{\bar{v}*}\,\tau_0^{-1} \tag{3-2}$$

---

[6] (a) OSRD 5611; (b) GMX-2 memorandum from W. W. Wood to L. C. Smith dated September 4, 1951.

[redacted] [redacted]

[redacted] [redacted]

TABLE 7

$N_A \bar{\epsilon}^*$ $\frac{\text{cal}}{\text{mole gas}}$	τ_0	τ_0^{-1}	τ	τ^{-1}	τ/τ_0	θ	D $\frac{\text{m}}{\text{sec}}$	T °K	$P\bar{v}^*$ megabars x $\frac{\text{cm}^3}{\text{mole gas}}$
60	0.4500	2.222	0.3643	2.745	0.810	103.6	10981	3128	12.6
	.5500	1.818	.4330	2.309	.787	124.2	8787	3751	7.37
	.7100	1.408	.5385	1.857	.758	137.4	7054	4148	4.179
	1.0000	1.000	.7238	1.382	.724	145.7	5684	4400	2.203
	1.5000	0.6667	1.0365	0.965	.691	150.1	4724	4532	1.134
100	0.5000	2.000	0.4060	2.463	0.812	63.5	11205	3196	11.7
	.6250	1.600	.4920	2.033	.787	76.9	8713	3870	6.38
	.8250	1.212	.6239	1.603	.756	84.5	6881	4251	3.453
	1.1500	0.8696	.8308	1.204	.722	88.6	5604	4461	1.871
	1.4750	.6780	1.0350	0.966	.702	90.2	4976	4538	1.236
	1.8000	.5556	1.2357	.809	.686	91.0	4595	4579	0.9079
200	0.5000	2.000	0.4143	0.214	0.829	25.2	14062	2535	16.7
	.6000	1.667	.4870	2.053	.812	35.1	10920	3536	9.24
	.7500	1.333	.5897	1.696	.786	40.8	8503	4104	3.815
	.9300	1.075	.7081	1.412	.761	43.4	7052	4364	3.145
	1.6000	0.625	1.1315	0.884	.707	45.8	5114	4606	1.185
300	0.625	1.600	0.5111	1.957	0.818	23.5	11692	3541	9.84
	.74071	1.350	.5922	1.689	.800	27.0	9470	4069	5.90
	.90901	1.100	.7048	1.419	.775	29.0	7715	4385	3.63
	1.17647	0.8500	.8776	1.139	.746	30.3	6333	4568	2.137
	1.66667	.6000	1.1879	0.842	.713	30.9	5204	4663	1.152

[redacted] [redacted]

Thus when D_{exp} is plotted against τ_0^{-1}, we obtain a family of centered straight lines whose slope depends on the value assigned to the theoretical parameter $\bar{v}^*$. Accordingly, a plot of the calculated D and D_{exp} vs τ_0^{-1} on the same axes affords the desired comparison. Agreement would consist in acceptable coincidence of two curves, one from each family. Such a plot is shown in Figure 1. For convenience the density corresponding experimentally to a given detonation velocity is indicated on the right hand side of the figure. The solid horizontal lines indicate the extremes of the experimental region; the dashed ones the limits of the presently well defined experimental region as suggested by D. P. MacDougall. Figures 2 and 3 show respectively the dependence of the calculated C-J temperature and reduced density on τ_0^{-1}.

For each of the four values of $N_A\bar{\epsilon}^*$ we have chosen $\bar{v}^*$ so as to minimize

$$\sigma^2 = \frac{\int_{1.0}^{1.6} (D-D_{exp})^2 \, d\rho}{\int_{1.0}^{1.6} d\rho}$$

These values of $\bar{v}^*$ and the corresponding values of σ, as well as the resulting values of D, ρ, p and T as functions of ρ_0 are shown in Table 8. These numbers were read off graphs constructed from Table 7, and are not as accurate as the latter. The value of σ is seen to decrease with decrease in $N_A\bar{\epsilon}^*$, while $\bar{v}^*$ increases. The range of Tables 1 to 6 does not permit calculation for $N_A\bar{\epsilon}^* < 60 \frac{\text{cal}}{\text{mole}}$ at present. It may be suspected that $\bar{v}^*$ will approach ∞ as $N_A\bar{\epsilon}^*$ approaches zero; the behavior of σ is harder to predict. It seems unlikely that σ will decrease below 100 m/sec., but detailed calculations would be required to prove this.

Figure 4 is a graph of $D - D_{exp}$ vs ρ_0 for these optimum pairs (the $N_A\bar{\epsilon}^*$ = 200 curve falls between those for 100 and 300; it is not shown in the figure to avoid confusion). From this figure it seems unlikely that substantial

[redacted]

[redacted]

[redacted] [redacted]

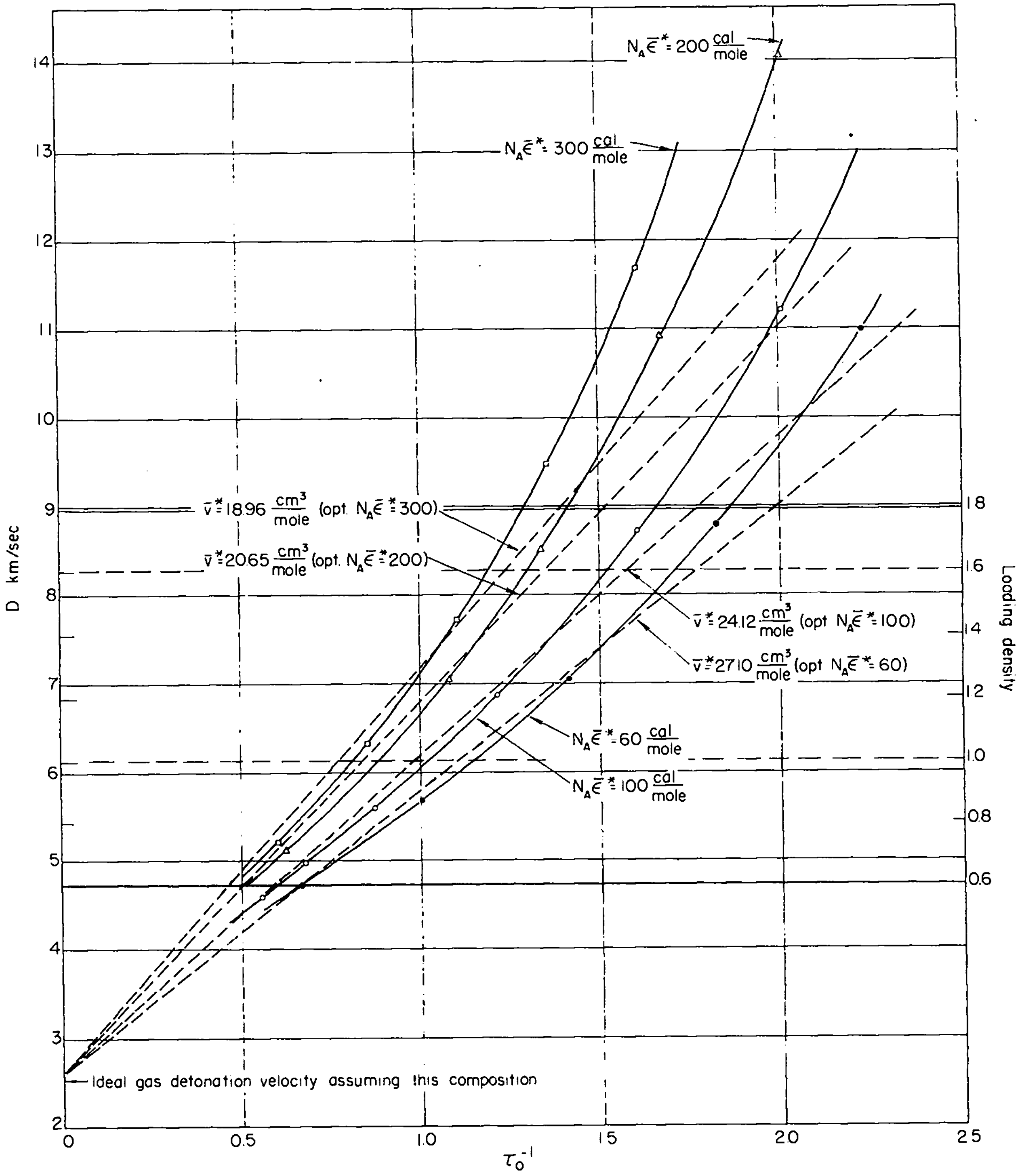

Figure 1. Detonation velocity vs. reduced loading density. Solid curves theoretical, dashed curves experimental.

[redacted] [redacted]

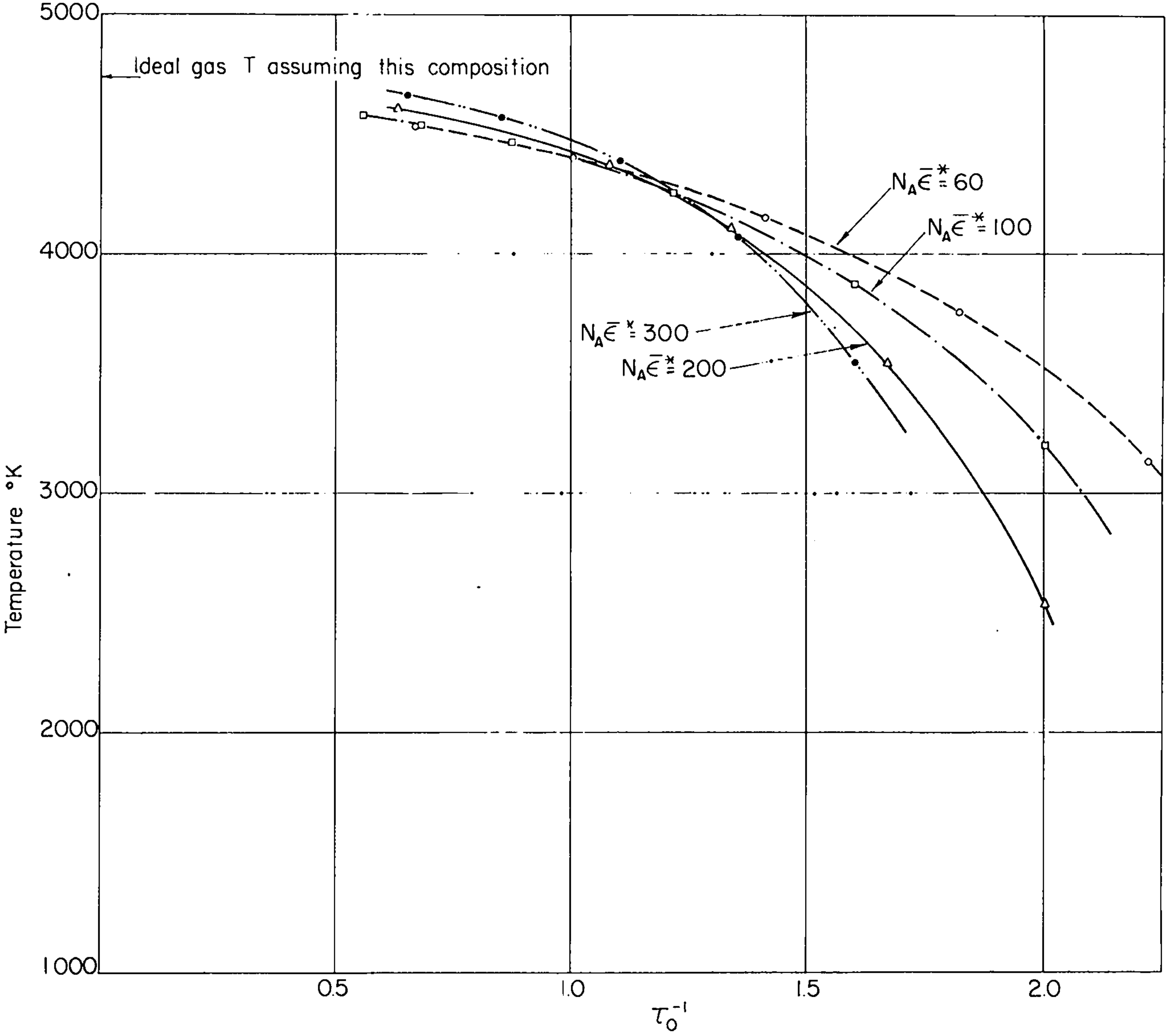

Figure 2. Chapman-Jouget temperature vs. reduced loading density.

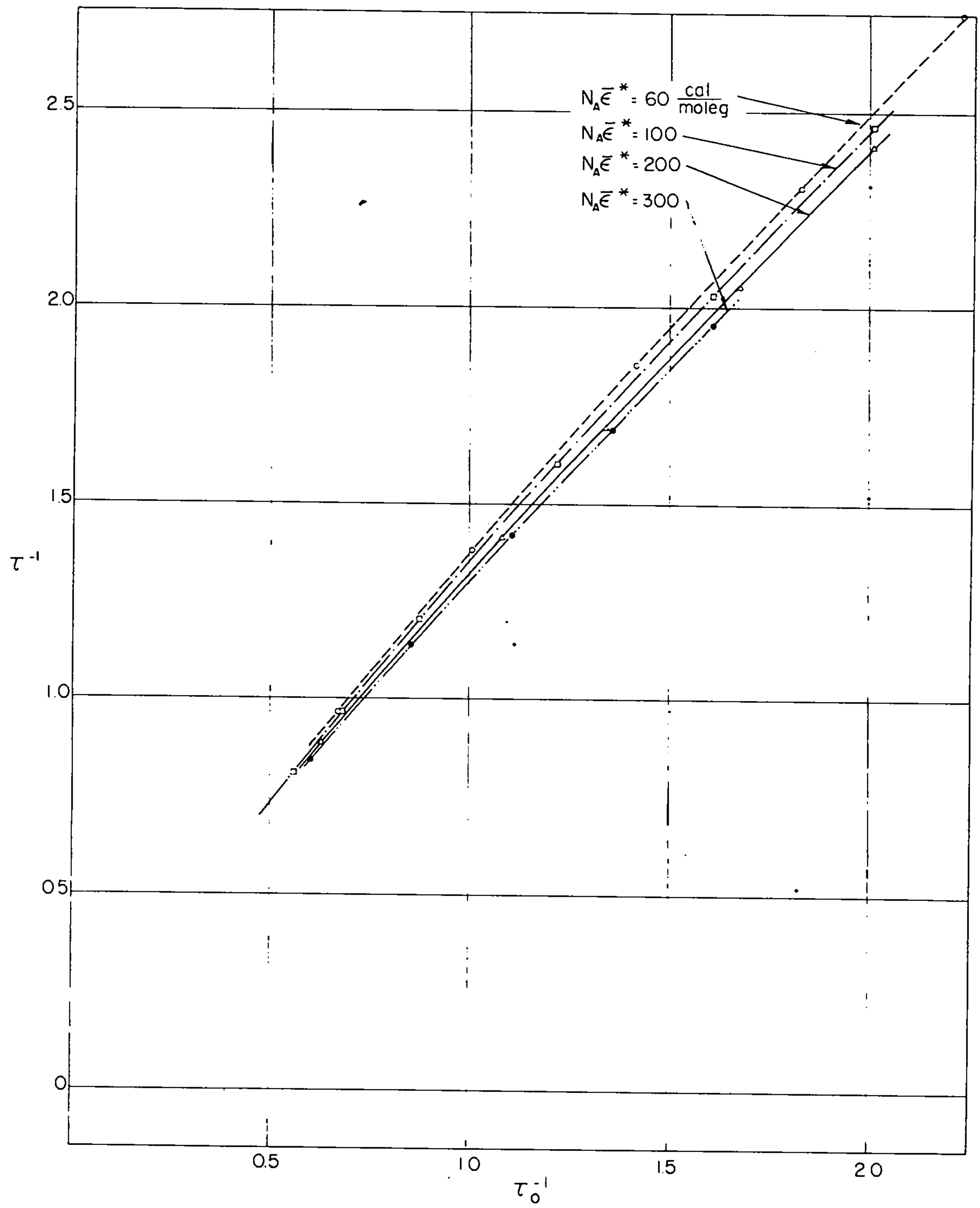

Figure 3. Chapman-Jouget reduced density vs. initial reduced density.

~~RESTRICTED~~
~~SECURITY INFORMATION~~

~~OFFICIAL USE ONLY~~

[redacted] [redacted]

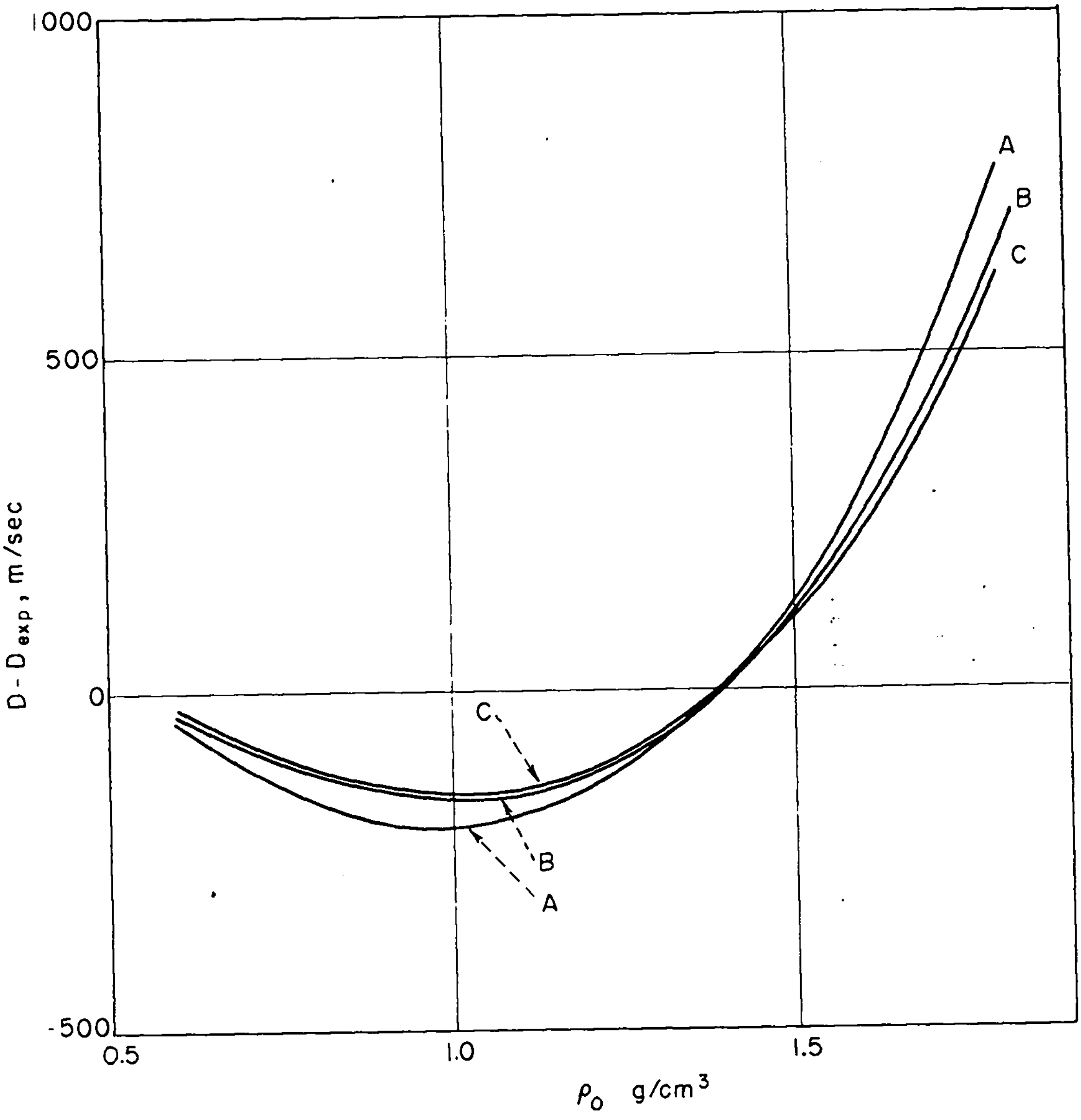

Figure 4. Deviation plot, detonation velocity vs. loading density. A, $N_A\bar{\epsilon}^* = 300 \frac{cal}{mole}$, $\bar{v}^* = 18.96 \frac{cm^3}{mole}$; B, 100 and 24.12; C, 60 and 27.10, respectively.

[redacted] [redacted]

TABLE 8

$\overline{N_A}^*$ cal/mole	$\bar{v}^*$ $\frac{cm^3}{mole}$	σ m/sec		ρ_0 g/cm³						
				0.6	0.8	1.0	1.2	1.4	1.6	1.8
60	27.10	118	D, m/sec	4700	5315	5990	6730	7555	8500	9590
			ρ, g/cm³	0.870	1.124	1.366	1.599	1.824	2.044	2.262
			P, mb.	0.0411	0.0651	.096	0.136	0.186	0.251	0.338
			T, °K.	4538	4452	4352	4217	4040	3822	3543
100	24.12	125	D	4685	5310	5980	6725	7555	8520	9620
			ρ	0.867	1.120	1.365	1.595	1.820	2.040	2.255
			P	0.0406	0.0644	.096	0.134	0.184	0.251	0.336
			T	4570	4505	4407	4281	4123	3916	3638
200	20.65	143	D	4685	5280	5945	6705	7565	8545	9680
			ρ	0.868	1.118	1.359	1.590	1.814	2.033	2.247
			P	0.0407	0.0634	0.093	0.132	0.183	0.249	0.336
			T	4646	4590	4517	4416	4282	4095	3845
300	18.96	151	D		5270	5940	6705	7575	8560	9740
			ρ		1.119	1.359	1.588	1.812	2.029	2.245
			P		0.0633	0.093	0.132	0.183	0.248	0.338
			T		4661	4606	4527	4400	4243	4015
Experimental D from equation (3-1)				4721	5429	6137	6845	7553	8261	8969

[redacted]

[redacted]

improvement would be obtained with smaller $N_A\bar{\epsilon}^*$. The uncertainity of the experimental data makes difficult a definite decision as to how well the present calculations agree with experiment. We are inclined to believe that the apparent disagreement is genuine, but have postponed a definite decision pending completion of the current experimental investigation, since it is clear that the high density region is of particular interest in this connection.

It is of interest to note that the pair of values $N_A\bar{\epsilon}^* = 224 \frac{\text{cal}}{\text{mole}}$, $\bar{v}^* = 25.48 \frac{\text{cm}^3}{\text{mole}}$ calculated from the L-J potential parameters obtained from low temperature virial coefficients lead to extreme disagreement in detonation velocity throughout the loading density region. The significance of this is obscured by the uncertainity in the intermolecular potential of water, as discussed in reference (1). However, not all the blame can be put on water, at least not if we continue to assume a L-J potential for it. This is evident from the fact that if one takes for N_2 and CO their second virial coefficient values ($\frac{\epsilon^*}{k} = 95.2°\, K$, $v^* = 29.9 \frac{\text{cm}^3}{\text{mole}}$ will suffice for both) and for the averages $\bar{\epsilon}^*$ and $\bar{v}^*$ takes in succession the four best pairs of values, and then attempts to solve for the water parameters, one finds that there is no solution in any of the four cases. Evidently if our present assumptions are valid at all, the potential parameters for N_2 and CO will require appreciable modification.

[redacted] [redacted]

Section 4.

Expected Development of the Investigation

As mentioned in Section 3, an experimental program is under way in GMX-2 and GMX-8 to obtain precise detonation velocity data for RDX, especially in the high density region. It is believed that these results will be available in the near future. If, as we expect, the apparent divergence of calculation and experiment in the high density region is proved to be real, we must then seek the explanation. The results of the trinitrotriazidobenzene and hexanitrosobenzene experimental programs mentioned in reference (1) will of course be of considerable help in this connection, when obtained. Certain improvements in the theory suggest themselves, and are discussed below.

It is of intrinsic interest to examine the predictions of this equation of state under the assumption of chemical equilibrium at the C-J plane, instead of assuming a fixed composition. The appropriate equations will be given in the revision of reference (1) mentioned in the introduction. In taking this step we are of course confronted with the already mentioned difficulty of the uncertainty of the relevant Lennard-Jones potential parameters for some components such as H_2O, in particular, and possibly, in the region of intermolecular distances of interest, even for such components as CO and N_2. It is of course an open question whether the use of a spherically symmetric potential for H_2O and CO_2 will give a reasonable approximation. Furthermore, solid carbon is a possible component, and calculations with it present will require its equation of state. Estimates of the latter have been made in T division, and can be used here. At present we have made

[redacted]

[redacted]

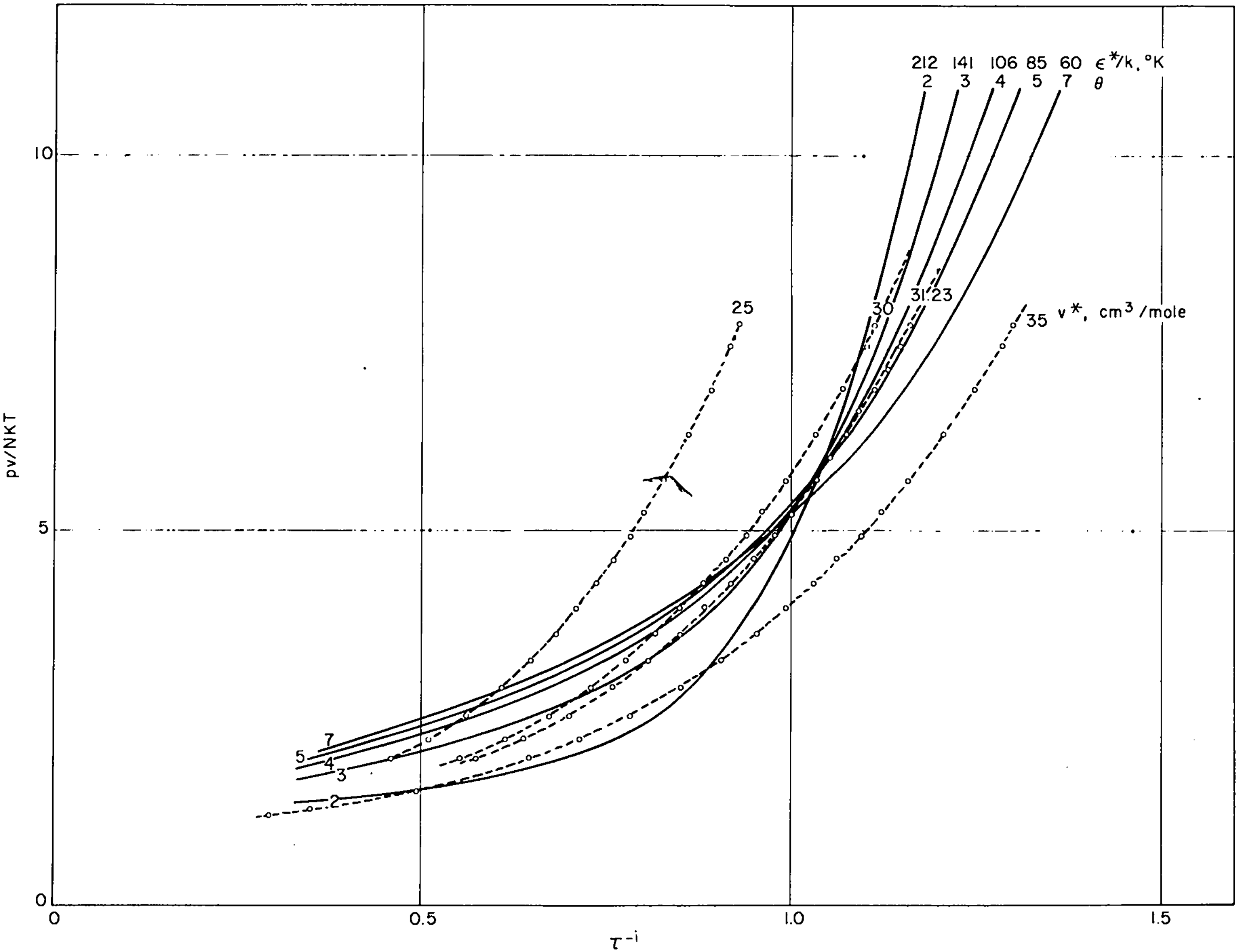

Figure 5. Theoretical and experimental pv/NkT vs. reduced density for N_2.

[redacted]

[redacted]

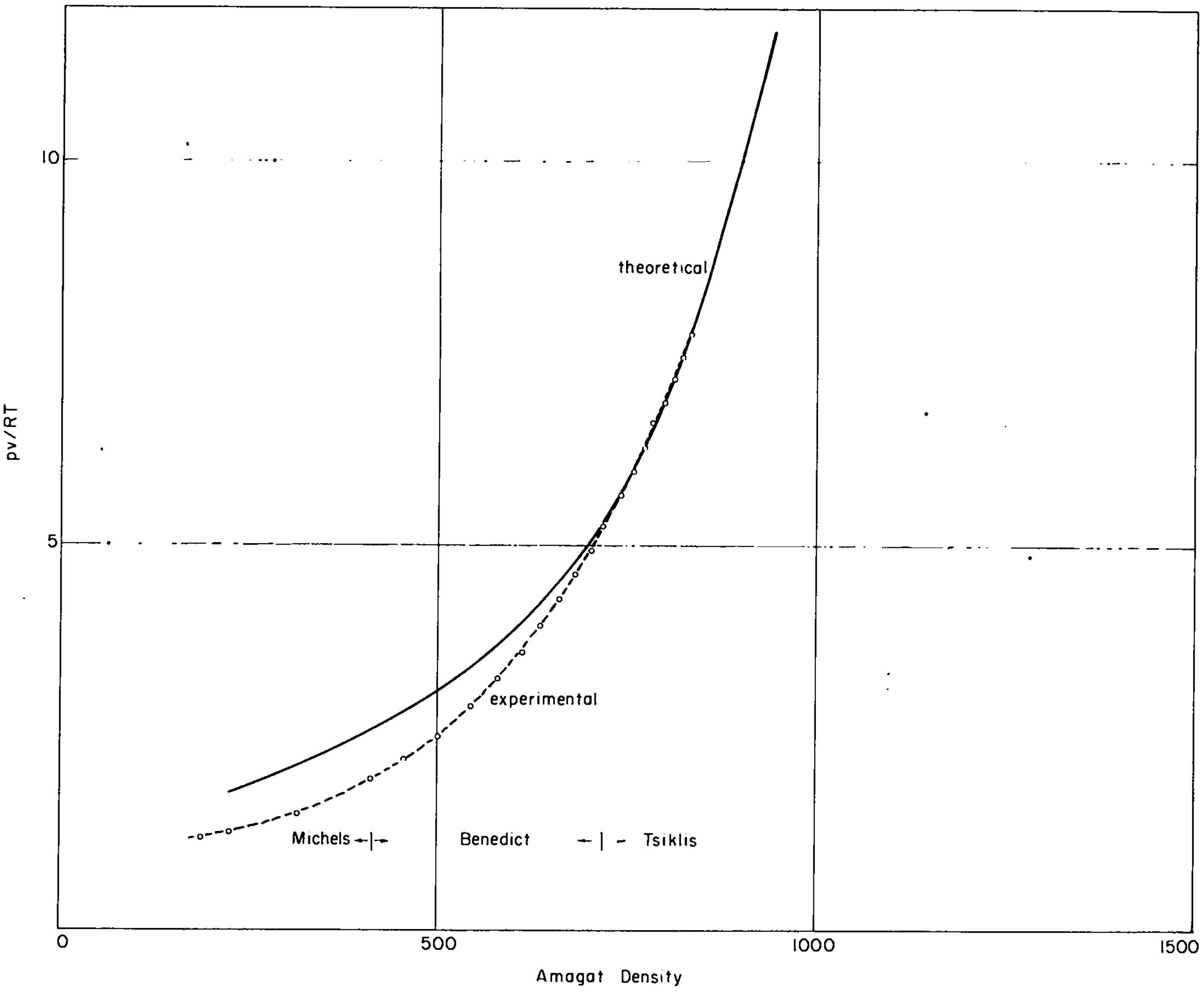

Figure 6. Theoretical and experimental pv/RT vs. Amagat Density for N_2.

[redacted]

only a single rough calculation for the reaction $H_2O + CO \rightarrow H_2 + CO_2$. Under conditions approximating the C-J point for RDX at 1.6 g/cm^3 loading density it was found that the equilibrium lay far to the left, with entirely negligible amounts of H_2 and CO_2. In this calculation the L-J parameters of Bird and Spotz[7] were used to compute the $v_{ij}^*/\bar{v}^*$ and $\Lambda_{ij}^*/\bar{\Lambda}^*$, while the values of τ and θ were approximately those for $N_A \bar{\epsilon}^* = 200$ cal/mole, $\bar{v}^* = 20.65$ cm^3/mole. We plan to make a more extensive investigation of the various possible equilibria in the near future.

A comparison of the ordinary L.J.D. free volume equation of state with low temperature, static high pressure measurements on N_2 is also of interest. Such a comparison was made by Wentorff, et.al.[2,8], but they did not use all the available experimental data[9]; in addition new data up to 10,000 atm. has recently appeared[10]. The older measurements of Bridgman[11] are apparently in error[9,10]. We have made a qualitative graphical comparison, shown in Figures 5 and 6. In Figure 5 we have chosen, as in Figure 1, τ^{-1} as the independent variable, and have plotted various theoretical L.J.D. isotherms of $\mathcal{P}$. The experimental isotherm chosen was for 150°C; with τ^{-1} as independent variable it becomes a family of curves with parameter v*. We seek a coincidence of two curves, one from each of the two families. The values $\epsilon^*/k = 92°K$, $v^* = 31.2 \frac{cm^3}{mole}$

---

[7] Bird and Spotz, University of Wisconsin Report CM-599, 1950; NOrd 9938; WIS-I-C.

[8] Michels, Wouters and de Boer, Physica, <u>3</u>,585 (1936)

[9] M. Benedict, J. Am. Chem. Soc.,<u>59</u>,2224 (1937); ibid.,<u>39</u>,2233 (1951)

[10] D. S. Tsiklis, Dokl. Akad. Nauk. U.S.S.R.,<u>79</u>(2),289-90 (1951)

[11] P. W. Bridgman, <u>Proc</u>. <u>Am</u>. <u>Acad</u>. Arts Sci.,<u>70</u>(1), (1935)

[redacted] [redacted]

[redacted]

are seen to result in rather good agreement for $\tau^{-1} > 1.0$, with increasing disagreement at lower densities, the theoretical values of ψ being too high. It is not possible to choose values outside this neighborhood which will give agreement over any appreciable interval in τ^{-1}. The values quoted are in rather good agreement with the values 91.5°K and 30.0 cm^3/mole found from viscosity measurements, and with the values 95.0°K and 30.5 cm^3/mole derived from second virial coefficient measurements[7]. One interpretation is that the L-J potential is possibly a good representation of the N_2 intermolecular potential over the corresponding range of intermolecular distances, the discrepancy at low density being due to the failure of one or more approximations in the theory. In Figure 6 the experimental and theoretical values of T are plotted against Amagat density, using the values ϵ^*/k = 91.5°K, v* = 31.2 cm^3/mole for the theoretical curve.

One is naturally led to inquire whether or not a correspondence can be set up which relates the experimental detonation region of temperature and density to a section of the low temperature isotherm of Figures 5 and 6. For a discussion of the validity of the theoretical approximations, an attempt to select values of temperature and volume such that the cell potential divided by kT is approximately the same function of the reduced cell radius r/a seems appropriate. That this should be possible, at least for high densities and under the assumption of the L-J potential, is suggested by the fact that for small τ the τ^{-4}/θ term in

$$\frac{W(r)}{kT} = 12\left[\frac{\tau^{-4}}{\theta}\,l\left(\frac{r^2}{a^2}\right) - 2\,\frac{\tau^{-2}}{\theta}\,m\left(\frac{r^2}{a^2}\right)\right]$$

will dominate, being assisted also by the dominance of $l(r^2/a^2)$ over $m(r^2/a^2)$. Consequently $\frac{W(r)}{kT}$, ψ, and ϵ'/θ, to a certain approximation, may be expected to depend on the single variable τ^{-4}/θ.

[redacted]

[redacted]

By actual computation of $w(r)/kT$ we find that such a correspondence can indeed be set up, with values in the neighborhood of those predicted by the preceding argument. Although admittedly rough it is believed that the argument has semi-quantitative validity. As a result we find that the upper limit of the detonation region ($\rho_0 = 1.8$ g/cm^3) corresponds to an Amagat density of 810 in Figure 5, while the lower limit (taken to be 0.8 g/cm^3) corresponds to density 400. It is interesting that the corresponding point of the upper limit occurs in the region of good agreement between experiment and theory, while for the lower limit, it is well into the region of disagreement. The suggestion is that if multiple occupancy, for instance, is important in the latter region at 150°C, then it may also be of importance in the lower loading density range in detonation. Conjectures about its importance in the former case have been made by others[2]. It should be noted that this discussion assumes, rather than proves or indicates, the validity of the L-J potential. Rather different intermolecular distances are in question in the two cases, and it is conceivable that at least part of the discrepancy in the detonation case may be due to this.

To date we have made only an exceedingly rough estimate of the departure from single occupancy, following the procedure of Janssens and Prigogine[12]. A very appreciable effect on $\mathcal{H}$ and $\mathcal{E}'$ for Θ and τ near the lower limit of the loading density range was indicated. A more thorough investigation of this point will be made.

If, as may be suspected from the preceding discussion, multiple

---

[12] P. Janssens and I. Prigogine, Physica 16, 895-906 (1950)

[redacted]

[redacted]

[redacted]

occupancy is becoming important in the lower loading density region, then it is also likely that the basic delta-function approximation to the molecules configurational distribution function $\varphi(r)$ in the cell may be breaking down at somewhat higher loading densities. Kirkwood[13] has suggested an iterative scheme of obtaining higher approximations to $\varphi(r)$, and we hope to investigate this point.

We also intend to examine the possibility of utilizing multiple occupancy as a conceptual tool in extending the present theory to molecules of different sizes.

In order to obtain numerical results from the theory in the region of present interest, it is necessary to specify the potential of intermolecular force for values of r/r_0 covering a range of about one-half to two. The presently available experimental information gives little more than a rough indication of the form of the potential in the high-energy part of this range.

The choice of the Lennard-Jones form for the intermolecular potential was made largely for the sake of mathematical convenience. The (6, 12) form has been used previously in this type of work, although present experimental evidence provides little, if any, reason for preferring it to the (6, 9) form.

The intermolecular potential of helium has probably been investigated more thoroughly than that of any other substance. Figures 7 and 8 show some of the proposed potential functions, both theoretical and experimental. The second virial coefficient of helium has recently been measured to 1200°C by Yntema and Schneider[14]. They attempted to determine from their data the

---

[13] J. G. Kirkwood, J. Chem. Phys. 18, 380-2 (1950)

[14] J. L. Yntema and W. G. Schneider, J. Chem. Phys., 18, 641 and 646 (1950)

[redacted] [redacted]

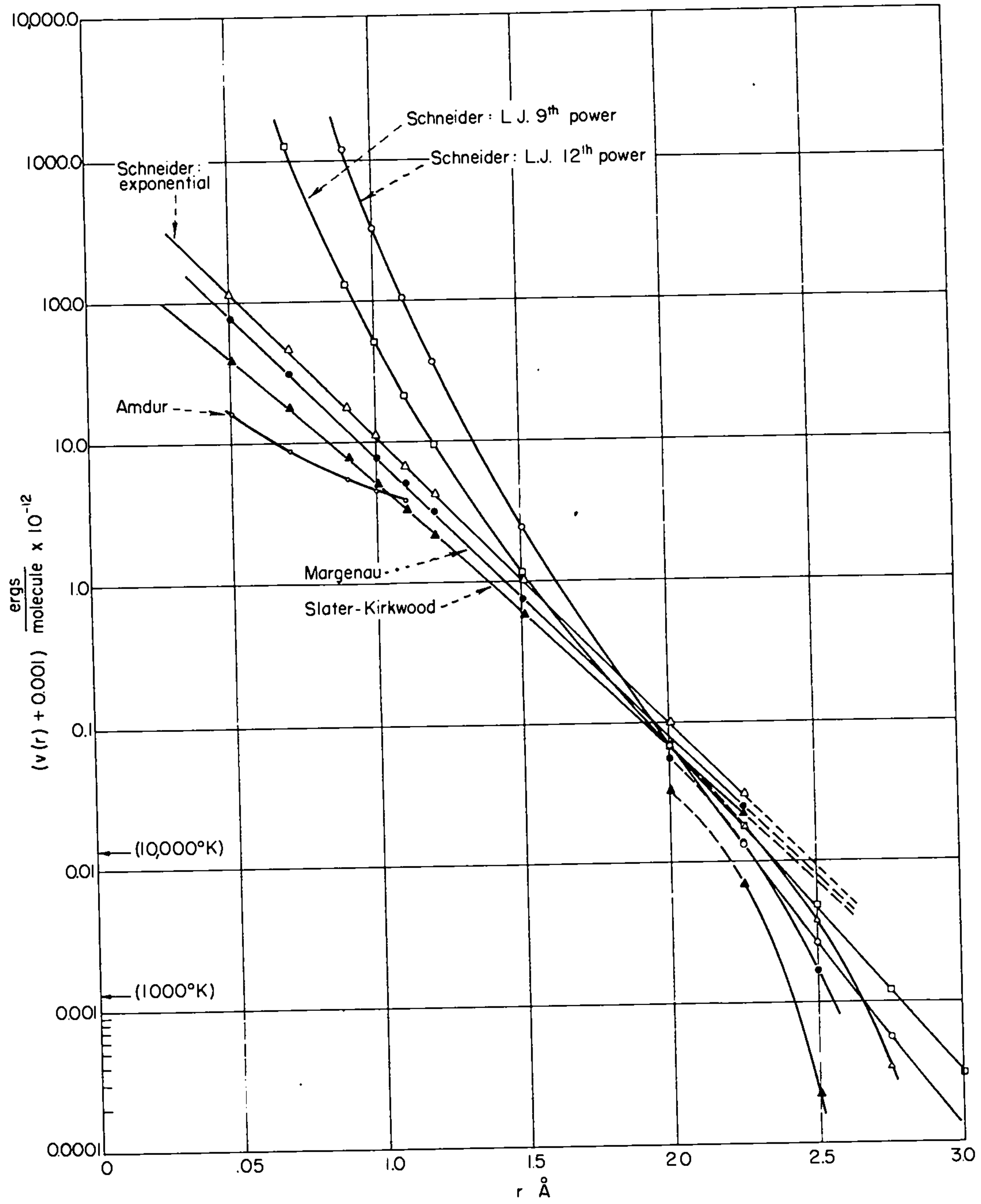

Figure 7. Potential energy curves for helium at distances less than r_0. For potentials with exponential repulsion, the portions of the curves above the break represent the repulsive terms only.

[redacted] [redacted]

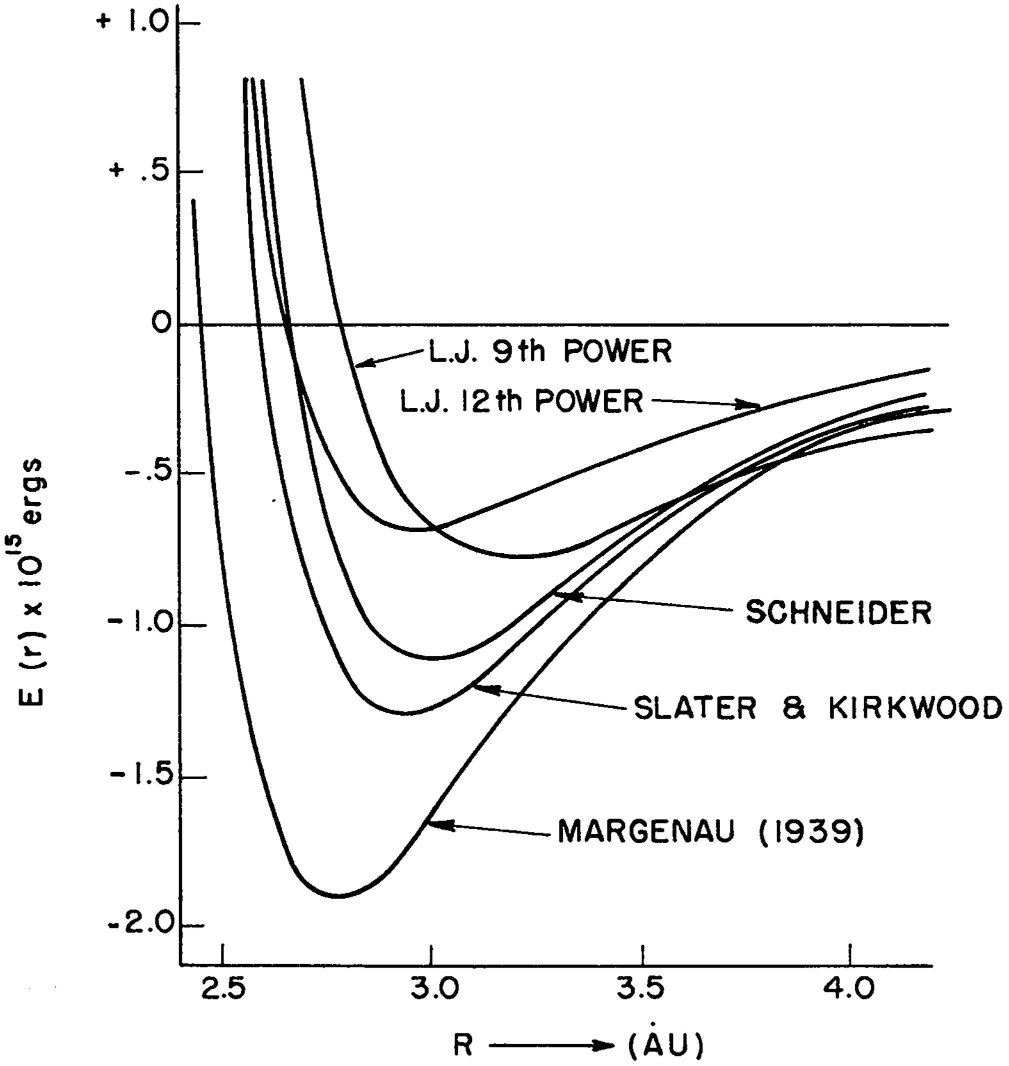

Figure 8. Potential energy curves for helium in the neighborhood of the minimum.[14]

as well as those in a form with exponential repulsion:

$$V(r) = b e^{-r/\rho} - \frac{c_1}{r^6} - \frac{c_2}{r^8}$$

The results indicated some preference for the exponential form, which could be made to reproduce the experimental second virial coefficient fairly well over the entire temperature range, although a divergence just exceeding the experimental error at the highest temperature suggests that the fit would become progressively poorer at higher temperatures. Of the two Lennard-Jones forms, a slight preference for the (6, 9) was indicated.

Margenau[15] and Slater and Kirkwood[16] have carried out quantum-mechanical calculations of the helium potential. Slater and Kirkwood calculate the repulsive term from first-order perturbation theory, then add an attractive term resulting from dispersion forces. Margenau[15] asserts that this type of approach is somewhat inconsistent, inasmuch as the repulsive force is calculated from first-order perturbation theory on wave-functions satisfying the Pauli exclusion principle, while the attractive force is calculated from second-order perturbation theory on wave-functions not satisfying the Pauli principle. Thus the attractive and repulsive terms calculated in this way may not be simply additive. His treatment claims consistency in this respect, for it uses a single set of wave-functions satisfying the Pauli principle and carries the perturbation treatment to second-order. His treatment claims reasonable validity at the minimum, but there is some doubt as to the validity of some of the later approximations at smaller distances.

The intermolecular potential at very small intermolecular distances

---

[15] H. Margenau, Phys. Rev., 56, 1000 (1939)

[16] J. C. Slater and J. Kirkwood, Phys. Rev., 37, 682 (1931)

has been determined from measurements of He-He collision cross-sections[17]. As shown in Figure 7, it lies somewhat below the other potentials, and has a somewhat different shape. This information is of no direct use to us, however, since it does not extend to sufficiently large intermolecular distances.

The curves presented in Figures 7 and 8 indicate that the intermolecular potential of the simplest rare gas is not well determined even in the neighborhood of the minimum, which exerts a considerable effect on the second virial coefficient at ordinary temperatures.

Figure 9 illustrates, in a rough way, the portion of the potential function which is important in determining the thermodynamic properties of the system. The two marked values for each τ and Θ indicate the ranges of intermolecular distance covered in the cell integration when $\mathcal{G}$, g_L, and g_M have reached approximately 90% or 99% of their final values. The pairs of values of τ and Θ given in Figure 9 correspond to the four corner pairs of values of τ and Θ in our double entry tabulation of the reduced equation of state.(Tables 1-6) The ranges of τ and Θ covered in the detonation calculation can be found in Table 7. In considering the implications of Figure 9 with respect to the importance of the shape of the potential function it must be remembered that the contribution to the compressibility, $\mathcal{H}$, of terms containing the integrals $\mathcal{G}$, g_L, and g_M, depends markedly on the values of τ and Θ. The compressibility is given by

$$\mathcal{H} = \{1 - \frac{12}{\theta}[2.4090\,\tau^{-2} - 2.0219\,\tau^{-4}]$$

$$- \frac{48}{\theta}[\tau^{-2} g_M/6 - \tau^{-4} g_L/6]$$

---

[17] I. Amdur, D. E. Davenport, and M. C. Kells, J. Chem. Phys., 18, 525 (1950)

[redacted]

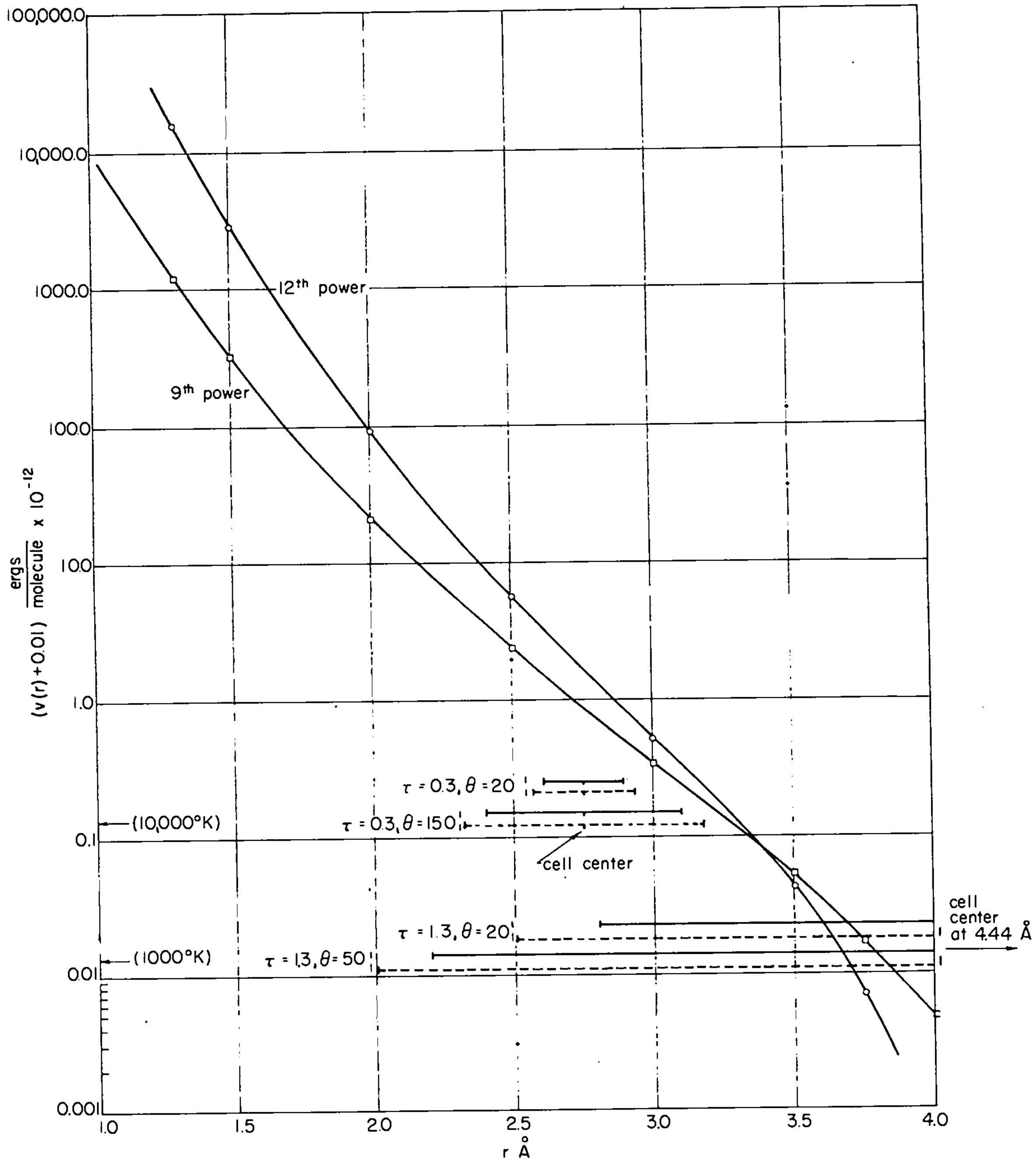

Figure 9. Lennard-Jones potential energy curves for nitrogen showing the intervals of intermolecular distance determining the thermodynamic properties.

[redacted]

[redacted]

For $\tau = 0.3$, $\theta = 20$ the term containing the integrals contributes about 10% of the value of $\mathcal{H}$; for $\tau = 1.3$, $\theta = 150$ the contribution of this term is well above 50% of the final value. The situation is complicated by the presence of the second term. For the low density-high temperature portion of the region covered by our tables, the integrations extend over wide ranges of internuclear distance and $\mathcal{H}$ is dominated by the third term. For high densities and low temperatures the second term, which is related to the energy of the molecule at the center of the cell, dominates; the third, which takes into account both the energy of the molecule at the center of the cell and what might be described as the "local shape" of the potential, is relatively unimportant. Thus the form of the potential and the values of its parameters influence the result in a rather complicated way. The situation with regard to the imperfection energy ϵ' is similar.

Because of the manifest uncertainty in the potential function, we plan to carry out calculations of the equation of state for the Lennard-Jones (6, 9) form, and probably also for a potential function of the form $V(r) = \left(\frac{6}{\alpha-6}\right)(\epsilon^*)\left[e^{-\alpha\left(\frac{r}{r_0}-1\right)} - \frac{\alpha}{6}\left(\frac{r_0}{r}\right)^6\right]$. The equation of state from the latter potential function would be a function of the reduced variables θ and τ, defined as before, but would depend in addition on the value of the non-dimensional parameter α. We have written down the expressions for the integrals analogous to G, g_L, and g_M; the labor involved in the numerical integration for a given value of α appears to be about twice that which is required for the Lennard-Jones potential.

Because we expect the new data for RDX in the high density region to be available shortly, we have not yet considered the extension to other conventional explosives. Should substantial agreement be obtained for the former, we shall of course proceed to such an application.

[redacted]